Int. J. Heat Mass Transfer. Vol. 20, pp. 841–846. Pergamon Press 1977. Printed in Great Britain

THE EFFECT OF SOLUTE LAYERING ON LATERAL HEAT TRANSFER IN AN ENCLOSURE

R. A. WIRTZ
Mechanical and Industrial Engineering Department, Clarkson College of Technology, Potsdam, NY 13676, U.S.A.

(*Received* 31 *May* 1976 *and in revised form* 4 *November* 1976)

Abstract—The effect of the presence of stable layering of a solute on the heat transfer across an enclosure with differentially heated side walls is studied. The method of investigation employed is the finite difference simulation of the governing conservation equations for laminar free convection. For stable convecting systems, the convecting layers are found to behave as individual, low aspect ratio enclosures, with a consequent decrease in lateral heat transfer. The fluid in layered systems which are kinematically unstable upon heating is observed to penetrate the diffusive interface adjacent to heated (or cooled) side walls, leading to rapid mixing of the layers.

NOMENCLATURE

D_S, solute diffusivity;
D_T, thermal diffusivity;
g, gravitational acceleration;
h, layer height;
H, enclosure height;
Le, Lewis number;
Nu, Nusselt number;
NX, grid number in x direction;
NY, grid number in y direction;
Pr, fluid Prandtl number;
Ra, thermal Rayleigh number;
R_ρ, stability number;
S, solute concentration;
T, fluid temperature;
u, horizontal velocity;
v, vertical velocity;
x, horizontal coordinate;
y, vertical coordinate.

Greek symbols

α, coefficient of thermal expansion;
β, coefficient of fractional expansion due to solute;
ΔT, wall temperature difference;
ΔS_0, solute concentration difference between layers;
ν, kinematic viscosity;
ρ, fluid density;
ψ, stream function;
ω, fluid vorticity.

1. INTRODUCTION

RECENTLY, considerable attention has been directed toward the study of flow and transport processes driven by multi-component diffusion effects. These effects result when two or more fluid components with different diffusivities interact in a body force field. Examples of combinations which have been studied experimentally are heat–salt and salt–sugar systems with diffusivity ratios of approximately 100 and 3 respectively. Turner [1] has summarized much of this previous work. When the component with smaller diffusivity is destabilizing, the "salt finger" instability is often observed. An example would be the interaction between cool, fresh water overlayed with hot, saline water.

On the other hand, convective layering is often observed when the component with larger diffusivity is destabilizing. An example of this case would be the layer formation observed when a stably stratified saline solution, with continuous gradient, is heated from the side. Upon sufficiently strong lateral heating, well mixed convective layers, separated by diffusive interfaces containing large vertical gradients of temperature and concentration, will form. The stability limits for incipient layer formation in both wide [2, 3] and narrow [4–7] enclosures have been established. For both the narrow and wide gap cases adjacent, initially formed convective layers merge two into one on a time scale which is approximately h^2/D_T with h the layer height and D_T the thermal diffusivity. Thus, a two-dimensional convective layer system evolves into a system of well mixed deep convecting layers separated by diffusive interfaces.

In this work we are interested in investigating how the lateral heat transfer across an enclosure is effected by the presence of solute stratifications as found in a layered system. Furthermore, under what conditions will the interface separating convecting layers become unstable resulting in merging. The method used is the finite difference simulation of the governing conservation equations assuming two-dimensional flow subject to the Boussinesq approximation. Because of layer merging the problem under study has no steady state solution and must be treated as an initial value problem. We have carried our calculations through the initial transient, out to where the flow kinetic energy is slowly varying, indicating a quasi-steady condition.

Previous numerical treatments dealt with layer for-

mation in an initially quiescent and linearly stratified fluid using explicit finite difference techniques [7, 8]. It was difficult to assess the effect of the presence of convecting layers on the lateral heat transfer since the numerical solutions became unreliable once convection was established. In this work an implicit alternating direction technique of solution has been employed. Rather than deal with a continuously stratified solution, we have fixed the number of convecting regions and the location of the diffusive interface separating them by considering an initially quiescent and isothermal fluid having a step change in solute concentration at enclosure midheight.

In Section 2 we describe the governing equations, boundary conditions and solution algorithm employed. This is followed in Section 3 with a survey of results which we have obtained for the lateral heating of a saline solution in a square enclosure. Finally, in Section 4 we summarize our conclusions.

2. ANALYSIS

The geometry considered consists of a rectangular enclosure of height, H and width, W with vertical side walls. The flow is assumed to be two-dimensional, in the x, y plane, having horizontal and vertical velocity components u, and v. Initially the fluid is isothermal at some mean temperature T_0 with a step decrease in salinity of magnitude ΔS_0 at enclosure midheight. The two side walls are suddenly changed to $T_0-(\Delta T/2)$ and $T_0+(\Delta T/2)$, while the top and bottom are adiabatic. All surfaces are impermeable to S and the no-slip condition on fluid velocity is applied. If the fluid has a linear state equation

$$\rho = \rho_0\{1-\alpha(T-T_0)+\beta(S-S_0)\}. \tag{1}$$

Then subject to the Boussinesq approximation the conservation equations may be written in dimensionless form as

$$\frac{\partial\bar{\omega}}{\partial\bar{t}} = -J(\bar{\omega},\bar{\psi})+Pr\nabla^2\bar{\omega}+RaPr\left[\frac{\partial\bar{T}}{\partial\bar{x}}-R_\rho\frac{\partial\bar{S}}{\partial\bar{x}}\right] \tag{2}$$

$$\frac{\partial\bar{T}}{\partial\bar{t}} = -J(\bar{T},\bar{\psi})+\nabla^2\bar{T} \tag{3}$$

$$\frac{\partial\bar{S}}{\partial\bar{t}} = -J(\bar{S},\bar{\psi})+\frac{1}{Le}\nabla^2\bar{S} \tag{4}$$

$$\nabla^2\bar{\psi} = -\bar{\omega} \tag{5}$$

with

$$\bar{\omega}=\frac{\partial\bar{v}}{\partial\bar{x}}-\frac{\partial\bar{u}}{\partial\bar{y}},\quad \bar{u}=\frac{\partial\bar{\psi}}{\partial\bar{y}},\quad \bar{v}=\frac{\partial\bar{\psi}}{\partial\bar{x}}. \tag{6}$$

All quantities have been non-dimensionalized using the enclosure width, W, as the characteristic length and W^2/D_T as the characteristic time. The dimensionless temperature and concentration are given by

$$\bar{T}=\frac{T-T_0+\dfrac{\Delta T}{2}}{\Delta T},\quad \bar{S}=\frac{S-S_0}{\Delta S_0}. \tag{7}$$

Equation (2) is a vorticity transport equation formed by combining the x and y momentum equations and application of equation (1). Equations (3) and (4) are heat and solute transport equations and equation (5) is the relation between stream function and vorticity which results when the two-dimensional stream function, ψ, is introduced to eliminate the incompressibility condition. $R_\rho \equiv \beta\Delta S_0/\alpha\Delta T$ is a stability number which is a measure of the ratio of density changes due to the stabilizing effect of the solute stratification divided by the destabilizing effect of the wall temperature increase. $R_\rho < 1$ results in a kinematically unstable density distribution. $Ra = g(\alpha\Delta T/\nu D_T)W^3$ is the thermal Rayleigh number based on enclosure width and Pr, Le are the fluid Prandtl and Lewis numbers. Equations (2)–(5) are the systems to be solved using finite differences.

Boundary and initial conditions are:

Initial conditions:

$$\bar{\psi}(0,\bar{x},\bar{y}) = \bar{\omega}(0,\bar{x},\bar{y}) = 0 \tag{8}$$

$$\bar{T}(0,\bar{x},\bar{y}) = 0.5 \tag{9}$$

$$\bar{S}(0,\bar{x},\bar{y}) = \begin{cases} 0, 0.5 < \bar{y} \leqslant 1 \\ 1, 0 \leqslant \bar{y} < 0.5 \end{cases} \tag{10}$$

Boundary conditions:

$$\bar{\psi}\left(\bar{t},\begin{matrix}0\\1\end{matrix},\begin{matrix}0\\\bar{H}\end{matrix}\right) = 0 \tag{11}$$

$$\bar{\omega}\left(\bar{t},\begin{matrix}0\\1\end{matrix},\bar{y}\right) = -\left.\frac{\partial^2\bar{\psi}}{\partial\bar{x}^2}\right|_{\bar{x}=0,1},\qquad \bar{\omega}\left(\bar{t},\bar{x},\begin{matrix}0\\\bar{H}\end{matrix}\right) = -\left.\frac{\partial^2\bar{\psi}}{\partial\bar{y}^2}\right|_{\bar{y}=0,\bar{H}} \tag{12}$$

$$\bar{T}\left(\bar{t},\begin{matrix}0\\1\end{matrix},\bar{y}\right) = \begin{matrix}0\\1\end{matrix},\left.\frac{\partial\bar{T}}{\partial\bar{y}}\right|_{\bar{y}=0,\bar{H}} = 0 \tag{13}$$

$$\left.\frac{\partial\bar{S}}{\partial\bar{x}}\right|_{\bar{x}=0,1} = 0,\quad \left.\frac{\partial\bar{S}}{\partial\bar{y}}\right|_{\bar{y}=0,\bar{H}} = 0. \tag{14}$$

Equations (2)–(4) were written in finite difference form, with all spatial derivatives second order accurate. In particular, the non-linear terms, J, of equations (2)–(4) were represented by centered differences. It is recognized that this discretized version of the Jacobian is non-conservative. However, it has been favorably compared to the Arakawa Jacobian representation, which is conservative to second order, for both viscous and nonviscous two dimensional, time dependent flows with only negligible difference in the results obtained [20]. This coupled with the simplicity of this representation as compared to Arakawa's form, dictated its use.

The finite difference equations were solved using the implicit alternating direction technique. The specific details of our algorithm are contained in [9]. In essence the IAD technique reduces the solution of equations (2)–(4) to the solution of $NX+NY$ tridiagonal systems of algebraic equations for each time step, where NX and NY are the number of grid points in the x and y directions respectively. We used the special form of Gauss-elimination for the solution of these tri-diagonal systems. In order to apply this to equations (2)–(4) we must apply the boundary conditions peculiar to each equation to the elements of the tri-diagonal system

which lie on the boundary. Application of the Dirichlet condition, and the zero normal derivative conditions on $\bar{T}$ and $\bar{S}$ are straightforward, the latter by applying symmetry to finite difference equations written about a boundary point. The vorticity boundary condition creates some difficulty since the boundary vorticity must be determined through extrapolation by application of finite differences to equations (6). Ultimately the boundary vorticity may be written in terms of adjacent grid point stream function values. We have used both first and second order accurate formulas which give essentially the same results.

The finite difference form of equation (5) had to be solved at each time step. Hockney's [10] Fourier Analysis and Cyclic Reduction scheme was used.

3. RESULTS

All calculations for stratified systems reported on here are for $Le = 100$ and $Pr = 6.7$ in order to simulate a thermohaline system. The region aspect ratio was held constant at $\bar{H} = 1$. Ra was varied between 5×10^4 and 10^6; R_ρ between 0 and 10. All calculations reported here are for a 17×17 grid, although we have performed a few 17×33 ($NX \times NY$) runs in order to ascertain if our grid was fine enough; the finer calculation led to essentially the same result as the 17×17 calculation. We also investigated the effect of varying the time step size on the calculation; $\Delta\bar{t}$ was varied between 4×10^{-5} to 10^{-2}. At higher R_ρ and Ra the larger time step size resulted in an oscillation in $\bar{S}$ and $\bar{T}$ in the y direction just above and below the diffusive interface. This is probably due to our use of centered differences for J_{xy} and could be minimized by decreasing $\Delta\bar{t}$.

As a check on our method we performed a few calculations for single component flows. The results are summarized in Table 1 where the average wall Nusselt number,

$$\overline{Nu} = \frac{1}{\bar{H}} \int_0^{\bar{H}} \frac{\partial \bar{T}}{\partial \bar{x}}\bigg|_{\bar{x}=0,1} \mathrm{d}\bar{y}, \tag{15}$$

Table 1. Overall Nusselt number in a square enclosure

Ra	Pr	$\overline{Nu}$
1.47×10^4	0.73	2.81
10^5	0.73	5.97
2.86×10^3	6.98	1.51
10^5	6.70	6.72
1.4×10^5	6.98	7.85

is calculated by numerical approximation to second order accuracy. Our results for air ($Pr = 0.73$) are in excellent agreement with those of Wilkes and Churchill [11] (for $Ra/Pr > 2 \times 10^4$), DeVahl Davis [12] and Newell and Schmidt [13] while they are higher than those of McGregor and Emery [14] and Quon [15]. Part of this variation in results might be attributable to a Prandtl number effect (both [14] and [15] were for $Pr = 1$). It has been shown that the effect of Prandtl number variation should be negligible at $Pr > 7$ [15].

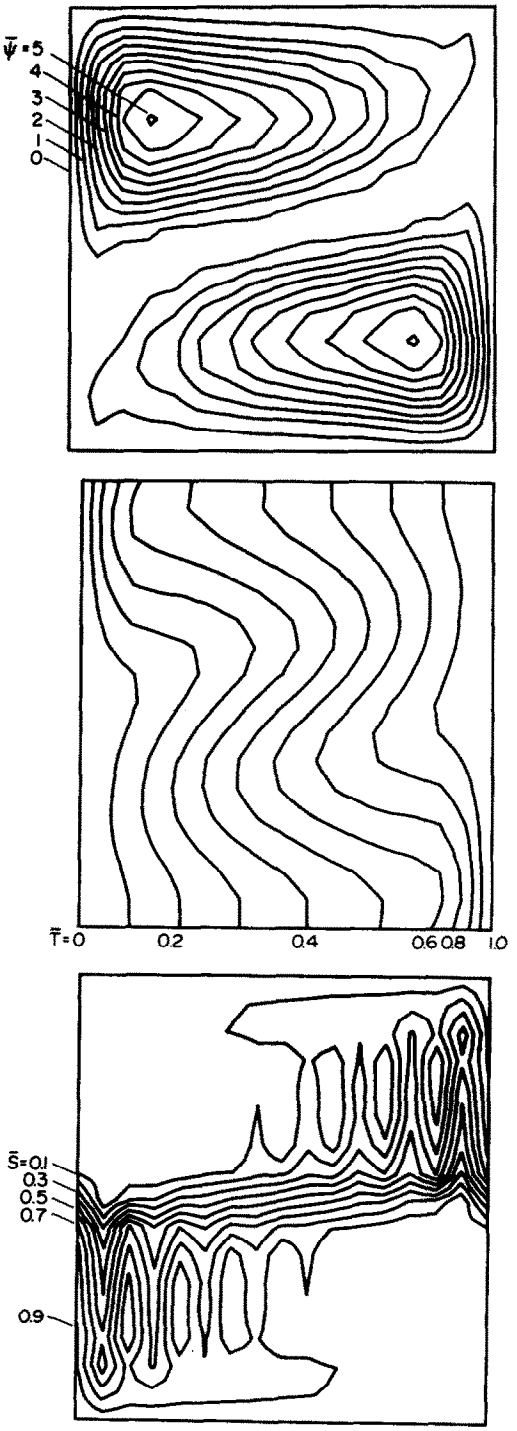

FIG. 1. Stream function temperature and solute isocontour maps at $Ra = 10^5$, $R_\rho = 2$ and $\bar{t} = 0.07$.

Our results for $Pr \simeq 6.8$ appear to agree well with those of DeVahl Davis ($Pr = 10$), but are 15–20% higher than those of Quon ($Pr = 7.14$) and Cormack *et al.* [16], ($Pr = 6.98$). All of the results noted stem from numerical calculations similar to ours, but it must be conjectured here that the variations are caused by seemingly minor differences in the numerical methods used. For example, [13] and [16] used a graded mesh via a transformation of coordinates, [15] used a staggered mesh with some grid points straddling the

boundaries and [11, 12, 14] and the present work used a uniform grid. References [15] and [16] considered conservative schemes while the others did not. Other less obvious differences, including the method of specification of boundary conditions, exist.

Figure 1 are stream function, temperature, and salinity isocontour maps for $Ra = 10^5$, $R_\rho = 2$, $Pr = 6.7$, and $\bar{t} = 0.7$. Two convecting regions, separated by a dead region are evident. Consider the upper convecting region. The isotherms (Fig. 2b) tend to be bunched near the left (cooled) wall while they are spread out near the right (heated) wall. A symmetric behavior is exhibited in the thermal field for the lower region. Cormack *et al.* [16], in the study of convection in shallow cavities, found that the character of the flow changed as the region aspect ratio was decreased to values much less than unity, departing from a boundary layer structure, and approaching a "parallel flow" structure where the flow is driven by the lateral temperature gradient existing in the core. Evidently, the same effect is exhibited in Fig. 1. The upper convecting region aspect ratio is approximately 0.55 near the cool wall and 0.35 near the heated wall. Thus the tendency toward a boundary layer structure is observed near the cool wall while flow driven by a uniform lateral temperature gradient exists near the heated wall.

Figure 1(c) shows a salinity isocontour map. The isohalines have been bunched together near the region midheight, indicating an interface region with large $\bar{S}$-gradient. The interface is inclined at an angle to the horizontal, the angle increasing with increasing Ra and decreasing R_ρ until overturning. Note the spires of constant salinity protruding into the convecting regions. A structure similar to this was observed with turbulent experiments reported in [17]. Either parcels of high salinity fluid are entrained along the diffusive interface, or a portion of the energetic flow from the boundary layer below penetrate the interface adjacent to the vertical walls. These are then convected across toward the cold wall where they settle, giving the "spire"

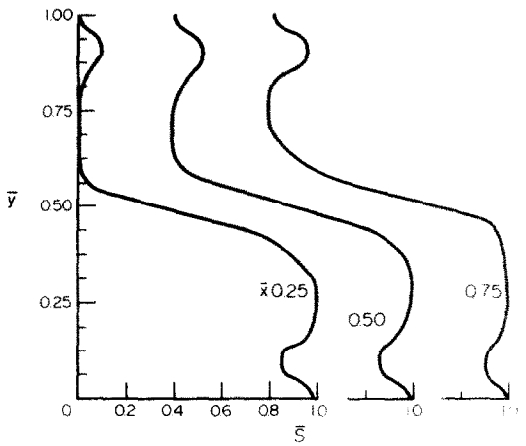

FIG. 2. Vertical solute profiles at $Ra = 10^5$, $R_\rho = 2$ and $\bar{t} = 0.07$.

appearance. Perhaps this effect is better displayed in Fig. 2, which plots vertical solute concentration profiles at three lateral locations for the conditions corresponding to Fig. 1.

We are interested in ascertaining the effect which the vertical salt stratification has on the lateral heat transfer. Figure 3 shows the transient wall Nusselt number (equation 15) at $Ra = 10^5$, $Pr = 6.7$ for $0 \leqslant R_\rho \leqslant 5$. Initially all curves follow the pure conduction curve. The homogeneous flow calculation departs from this at $\bar{t} \simeq 0.006$ and reaches a constant value of $\overline{Nu} = 6.7$. This transition is delayed with increasing R_ρ. For $R_\rho > 1$, the flow develops into the double convection mode as shown in Fig. 1. The Nusselt number is quasi-steady here, with a slow increase which would presumably continue as the salinity difference between the two regions is diminished through vertical diffusion across the interface. When the current value of $R_\rho = 1$, the interface would overturn.

The flow field for $R_\rho < 1$ is distinctly different as shown in Fig. 4 which are stream function, temperature and salinity maps for $Ra = 10^5$, $R_\rho = 0.75$ at

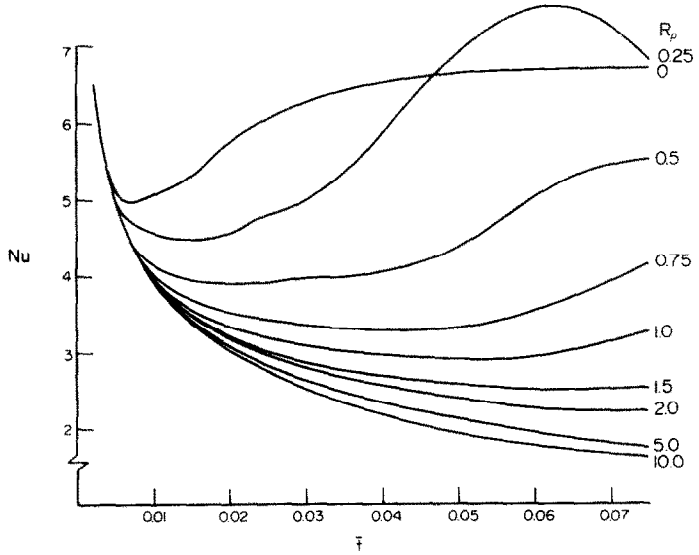

FIG. 3. Transient wall Nusselt number for $Ra = 10^5$ and $0 \leqslant R_\rho \leqslant 10$.

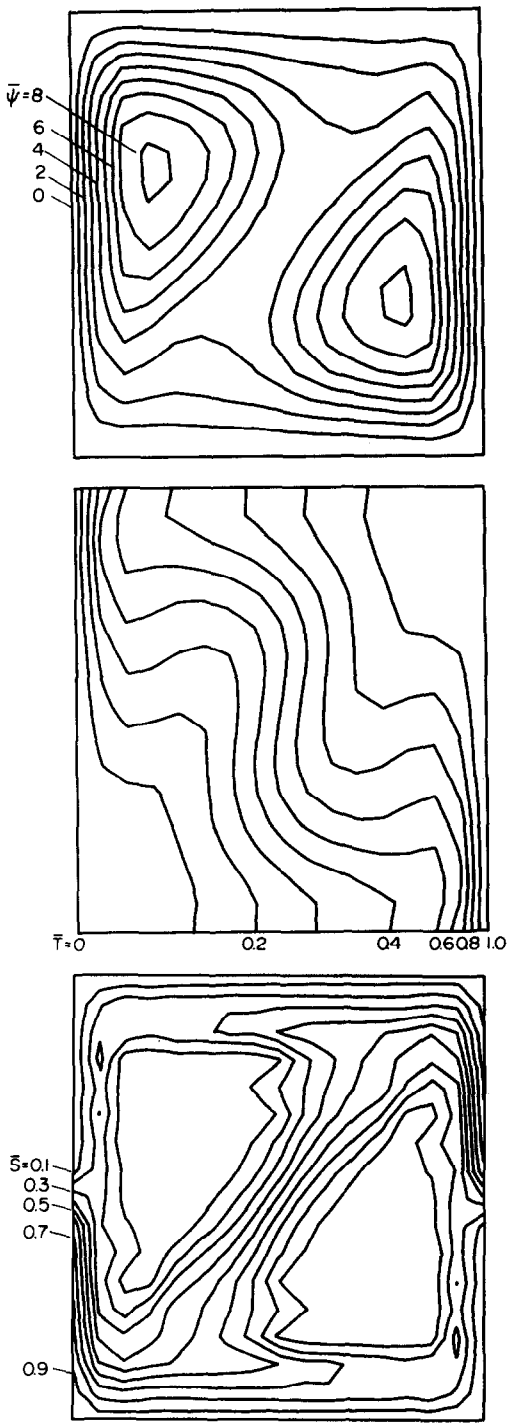

FIG. 4. Stream function, temperature, and solute isocontour maps at $Ra = 10^5$, $R_\rho = 0.75$ and $\bar{t} = 0.07$.

$\bar{t} = 0.07$. In this case fluid near the vertical wall penetrates the diffusive interface and begins to mix with fluid in the other convecting region. At this point our numerical simulation probably loses its validity since the actual mixing would probably be turbulent. The turbulent mixing process would serve to accelerate the system's return to the homogeneous fluid situation.

Figure 4(c) shows that the isohalines adjacent to the vertical walls at midheight have not moved from their original location even though the layers are overturning. This is a consequence of the no-slip and impermeable wall boundary conditions [equations (12) and (14)]. The thickness of these regions is probably not accurate, being magnified by the finite size grid used.

We have carried all calculations shown in Fig. 3 out to a time of $\bar{t} = 0.3$. This corresponds to a dimensional time of 5.56 h for a 10 cm wide enclosure ($D_T = 1.5 \times 10^{-3}\,\text{cm}^2/\text{s}$). For all $R_\rho \leqslant 1$ the layers overturned at $\bar{t} < 0.07$. For all $R_\rho > 1$, the system remained stable, with the wall Nusselt number remaining near the lower values shown in Fig. 3.

Part of the decrease in wall Nusselt number shown in Fig. 3 for $R_\rho > 1$ occurs because a fraction of the vertical walls are covered by the interface region where lateral transport is predominately by conduction. Another part stems from changes in the character of the flow in the convecting region due to the presence of the diffusive interface. Consider Fig. 5, which is a comparison of the local Nusselt number along the heated wall for $R_\rho = 0$ and $R_\rho = 2$. For the stratified case the

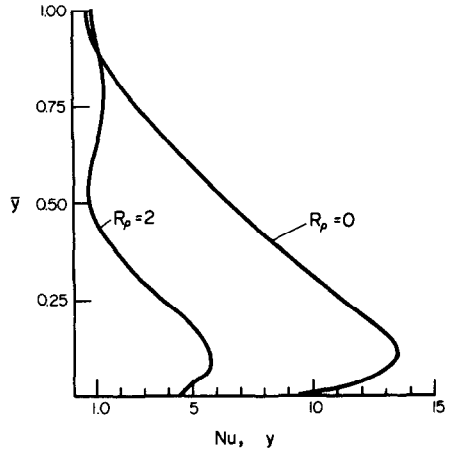

FIG. 5. Local wall Nusselt number at $Ra = 10^5$ for $R_\rho = 0$ and $R_\rho = 2$.

bottom convecting region extends to $\bar{y} \simeq 0.55$. The local heat-transfer coefficient exhibits the same variation in $\bar{y}$ as the $R_\rho = 0$ case, but at reduced magnitude. If we calculate $\overline{Nu}$ over the interval $0 \leqslant \bar{y} \leqslant 0.55$, we obtain an average value of 3.2. This is compared to a value of 2.7 obtained from Fig. 12 of [16] for a differentially heat cavity with $\bar{H} = 0.55$, $Pr = 6.98$ at the same Ra. The agreement obtained (the difference being 15%) is encouraging since our results for a square enclosure were also about 15–20% in excess of theirs. The characteristics of the Nu vs $\bar{y}$ curve for the upper region, $0.55 < \bar{y} < 1$, are even more like those of a low-aspect ratio cell, resulting in an average $\overline{Nu}$ determined to be 1.06. This decrease in $\overline{Nu}$ with decreasing aspect ratio for enclosures with $\bar{H} < 1$ has also been observed by Boyack and Kearney [18] and Sernas *et al.* [19] where the working fluid was air.

CONCLUSIONS

The major effect of the layering of solute is to decrease the heat transfer across the enclosure. At $R_\rho > 1$ each layer acts more or less like an individual

low aspect ratio cell. As the layer aspect ratio decreases, the flow field approaches the "core flow" configuration with its associated conduction temperature field as discussed in [16]. This appears to be the major reason for the reduction in overall Nusselt number. An additional reduction is obtained at wall locations adjacent to the diffusive interface separating convecting layers.

At $R_\rho < 1$, the diffusive interface separating convecting regions is kinematically unstable. Vertically moving fluid adjacent to the side walls penetrates the diffusive interface with consequent rapid mixing of the two layers.

Acknowledgements—Support for this work under sponsorship of The National Science Foundation under grants GK-37396 and ENG75-05337 is gratefully acknowledged. Mr. C. S. Reddy assisted through preparation of the computer code for the finite difference simulation.

REFERENCES

1. J. S. Turner, Double-diffusive phenomena, *A. Rev. Fluid Mech.* **6**, 37–56 (1974).
2. C. F. Chen, D. G. Briggs and R. A. Wirtz, Stability of thermal convection in a salinity gradient due to lateral heating, *Int. J. Heat Mass Transfer* **14**, 57–65 (1971).
3. C. F. Chen, Onset of cellular convection in a salinity gradient due to a lateral temperature gradient, *J. Fluid Mech.* **63**, 563–576 (1974).
4. J. A. Thrope, P. K. Hutt and R. Soulsby, The effect of horizontal gradients on thermohaline convection, *J. Fluid Mech.* **38**, 375–400 (1969).
5. J. E. Hart, On sideways diffusive instability, *J. Fluid Mech.* **49**, 279–288 (1971).
6. J. E. Hart, Finite amplitude sideways diffusive convection, *J. Fluid Mech.* **59**, 47–64 (1973).
7. R. A. Wirtz and L. H. Liu, Numerical experiments on the onset of layered convection in a narrow slot containing a stably stratified fluid, *Int. J. Heat Mass Transfer* **18**, 1299–1305 (1975).
8. R. A. Wirtz, D. G. Briggs and C. F. Chen, Physical and numerical experiments on layered convection in a density stratified fluid, *Geophys. Fluid Dynam.* **3**, 265–288 (1972).
9. R. A. Wirtz, The effect of lateral gradients on vertical gradient thermohaline convection, MIE Report No. 011, MIE Department, Clarkson College of Technology, Potsdam, NY 13676 (1975).
10. R. W. Hockney, The potential calculation and some applications, *Meth. Comput. Phys.* **9**, 135–212 (1970).
11. J. O. Wilkes and S. W. Churchill, The finite-difference computation of natural convection in a rectangular enclosure, *A.I.Ch.E. Jl* **12**, 161–166 (1966).
12. G. DeVahl Davis, Laminar natural convection in an enclosed rectangular cavity, *Int. J. Heat Mass Transfer* **11**, 1675–1693 (1968).
13. M. E. Newell and F. W. Schmidt, Heat transfer by laminar natural convection within rectangular enclosures, *J. Heat Transfer* **92**, 159–168 (1970).
14. R. K. MacGregor and A. F. Emery, Free convection through vertical plane layers—moderate and high Prandtl number fluids, ASME paper No. 68-WA/HT-4 (1969).
15. C. Quon, High Rayleigh number convection in an enclosure—a numerical study, *Physics Fluids* **15**, 12–19 (1972).
16. D. E. Cormack, L. G. Leal and J. H. Seinfeld, Natural convection in a shallow cavity with differentially heated end walls. Part 2. Numerical solutions, *J. Fluid Mech.* **65**, 231–246 (1974).
17. R. A. Wirtz and C. S. Reddy, Heat and mass transport across diffusive interfaces bounded by turbulent convecting regions, *Int. J. Heat Mass Transfer* **19**, 471–478 (1976).
18. B. E. Boyack and D. W. Kearney, Heat transfer by laminar natural convection in low aspect ratio cavities, ASME paper 72-HT-52 (1972).
19. V. Sernas, L. S. Fletcher and C. Rago, An interferometric study of natural convection in rectangular enclosures of aspect ratio less than one, ASME paper 75-HT-63 (1975).
20. D. G. Fox and J. W. Deardorff, Computer methods of simulation of multidimensional, nonlinear, subsonic, incompressible flow, ASME paper No. 72-HT-61 (1972).

EFFET D'UNE DISPOSITION EN COUCHES DE SOLUTE SUR LE TRANSFERT THERMIQUE LATERAL DANS UNE ENCEINTE

Résumé—On étudie l'effet de la présence d'une disposition en couches stables d'un soluté sur le transfert thermique dans une enceinte ayant des parois différemment chauffées. La méthode de recherche employée est la simulation aux différences finies des équations de conservation pour la convection naturelle laminaire. Pour des systèmes stables, les couches convectives se comportent comme des enceintes individuelles à faible rapport de forme, avec, par conséquent une décroissance du transfert latéral. Dans les systèmes à couches cinématiquement instables, le fluide pénètre l'interface de diffusion adjacent aux parois chauffées (ou refroidies), ce qui conduit à un mélange rapide des couches.

DER EINFLUSS EINER LÖSUNGSSCHICHTUNG AUF DEN WÄRMEÜBERGANG QUER ZU DEN BEHÄLTERWANDUNGEN

Zusammenfassung—Es wird der Einfluß einer stabilen Schichtung des gelösten Stoffes auf den Wärmeübergang in einem Behälter mit unterschiedlich beheizten Seitenwänden untersucht. Die den Vorgang beschreibenden Erhaltungsgleichungen für laminare, freie Konvektion werden mit Hilfe eines Differenzenverfahrens gelöst. Bei stabilen Systemen verhalten sich die Konvektionsschichten wie einzelne, niedrige Behälter mit entsprechender Abnahme des Wärmeübergangs in Querrichtung. In geschichteten Systemen, welche bei Beheizung kinematisch instabil werden, wurde ein Eindringen des Fluids in die Diffusionsgrenzfläche an den beheizten (oder gekühlten) Seitenwänden beobachtet, was zu einer raschen Vermischung der Schichten führte.

ВЛИЯНИЕ ПРОСЛОЕК РАСТВОРЕННОГО ВЕЩЕСТВА НА ТЕПЛООБМЕН ЧЕРЕЗ БОКОВЫЕ СТЕНКИ ПОЛОСТИ

Аннотация — Изучается влияние стабильных прослоек растворенного вещества на теплообмен в полости с различно нагретыми боковыми стенками. Исследование проводилось с помощью конечно-разностного метода решений уравнений сохранения для ламинарной естественной конвекции. Найдено, что в стабильных теплопередающих системах передающие слои ведут себя как самостоятельные включения с ослабленным теплообменом через боковые стенки. Наблюдалось, что жидкость в слоистых системах, кинематически нестабильных при нагревании, проникает через диффузионную поверхность раздела, граничащую с нагретыми (или холодными) боковыми стенками, и приводит к быстрому перемешиванию слоев.